Molecular Origins of Wettability of Hydrophobic Poly(vinylidene fluoride) Microporous Membranes on Poly(vinyl alcohol) Adsorption: Surface and Interface Analysis by XPS

Shubhangi G. Gholap and Manohar V. Badiger*

Polymer Science and Engineering Division, National Chemical Laboratory, Dr. Homi Bhabha Road, Pune 411 008, India

Chinnakonda S. Gopinath*

Catalysis Division, National Chemical Laboratory, Dr. Homi Bhabha Road, Pune 411 008, India

Received: February 16, 2005; In Final Form: May 11, 2005

Irreversible adsorption of poly(vinyl alcohol) (PVA) on hydrophobic, porous poly(vinylidene fluoride) (PVDF) membranes was carried out using aqueous PVA solution. Water permeation was observed in PVDF microporous membranes after PVA adsorption, and maximum permeability was obtained after treatment with 4% PVA solution. Water permeability increased linearly with increasing PVA concentration up to 4%, and then a marginal decrease with a further increase in PVA concentration occurred. PVA adsorbed PVDF membranes were subjected to intense physicochemical analysis, especially with XPS. XPS results display the presence of an interface between PVA and PVDF, and the binding energy (BE) of the interface is low for the PVDF membranes treated with 4% PVA. Carbon from CF_2-groups and F 1s core level clearly showed a decrease in its content on the surface after PVA adsorption and showed a minimum fluorine content at 4% PVA. F 1s BE shifts by 0.5 eV upon PVA adsorption and is independent of PVA concentration. EDAX analysis indicates that the bulk oxygen content remains within 4.5 ± 0.6% and is independent of the PVA concentration. Nonetheless, a large amount of surface atom percentage of oxygen (20 ± 4%) from O 1s core level shows an increase in PVA content on the surface of PVDF, and it is restricted mostly to the surface. The 4% PVA treated PVDF membrane clearly shows a broadening of O 1s core level to lower BE and indicates the interaction between PVDF and PVA which is significantly different compared to any other compositions. A new valence band feature at low BE, which is nonexistent on PVDF, develops after PVA adsorption. This indicates that the shift in the nature of the highest occupied molecular orbital (HOMO) derived mostly from oxygen; simultaneously, a suppression in the PVDF derived band indicates the change in nature of the PVA adsorbed surfaces from hydrophobic to hydrophilic. The above observations also suggest an irreversible electronic interaction between PVA and PVDF, possibly through charge transfer.

1. Introduction

Applications of hydrophobic membranes in bioseparation are limited since they are susceptible for irreversible protein adsorption and fouling. There are several approaches, which have been reported to render membranes hydrophilic in nature by chemical modification,[1,2] plasma treatment,[3−7] and coating.[8−11] The modification involves the introduction of polar functional groups to the polymer surface by surface grafting, coupling reactions, and so forth.[12,13] However, the modification of fluoropolymers by chemical methods in particular is rather difficult because of their good chemical resistance. Therefore, alternative approaches have been explored.

Recently, the adsorption of hydrophilic polymers onto hydrophobic surfaces has attracted major attention although the concept of protein adsorption onto hydrophobic biological membranes was known much earlier. For example, to improve the wettability, adhesion, and chemical reactivity, the hydrophobic surface of a fluoropolymer, poly(tetrafluoroethylene-*co*-hexafluoropropylene) [FEP], film was modified by poly(L-lysine) [PLL] by a simple adsorption technique.[14] The adsorption characterizations were studied by X-ray photoelectron spectroscopy [XPS] and contact angle measurements. It was observed that PLL adsorbs only under certain conditions, at pH 11, when it exists in the ∝-helix conformation.

Although most of the synthetic water-soluble polymers do not adsorb onto hydrophobic surfaces, it has been shown that poly(vinyl alcohol) [PVA] spontaneously adsorbs onto hydrophobic substrates.[15−20] PVA is a highly hydrophilic, nontoxic, and biocompatible polymer with an excellent film-forming property. The films have high mechanical strength, low fouling potential, and long-term temperature and pH stability. These properties of PVA have led to their use in bioseparations. Kozlov et al.[15] have studied the adsorption of PVA onto different hydrophobic substrates, which include fluoropolymers, hydrophobic polyolefins, silicon wafers, and polyester films. They generalized the phenomenon of adsorption of PVA from the aqueous solution onto hydrophobic surfaces and hypothesized that the hydrophobic interactions or the displacement of water molecules from the hydrophobic solid water interfaces and crystallization drives the adsorption. Akashi et al.[16] have reported on the formation of multiple thin layers on the gold surface. Coupe and Chen[17] have examined the effect of PVA concentra-

* To whom correspondence should be addressed. M.V.B.: fax: 0091-20-2589 3041; e-mail: badi@che.ncl.res.in; C.S.G.: fax: 0091-20-2589 3761; e-mail: cs.gopinath@ncl.res.in.

10.1021/jp050806r CCC: $30.25
Published on Web 07/01/2005

tion on the kinetics of adsorption by XPS. Nash et al.[18] have reported on the adsorption of PVA onto poly(styrene-divinyl benzene) beads for use in affinity chromatography.

Despite the fact that PVA adsorption onto various hydrophobic surfaces has been extensively studied, the exact mechanism of irreversible adsorption of PVA onto hydrophobic porous substrates is yet to be fully understood. In the present work, we have studied the adsorption of PVA onto highly porous, hydrophobic poly(vinylidene fluoride) (PVDF) membranes. The improved wettability of the hydrophobic PVDF membranes was investigated by water flux and contact angle measurements. The incorporation of PVA onto PVDF membranes was confirmed by XPS and EDAX studies. The influence of concentrations and molecular weights of PVA adsorption on PVDF was also investigated by XPS. XPS studies clearly showed a surface domination of PVA with the formation of interface between PVA and PVDF. Further, the energy and nature of the highest occupied molecular orbital (HOMO) of PVDF changes to lower binding energy and oxygen derived, respectively, upon PVA adsorption, which could be the origin of wettability.

2. Experimental Section

2.1. Preparation of PVA Adsorbed PVDF Membranes. Poly(vinyl alcohol) was procured from Fluka, with MW 31 000 and 67 000, and the degree of hydrolysis is in the range of 86.7−88.7 mol %. The hydrophobic porous PVDF membranes with pore size of 0.45μm were purchased from Millipore. PVA solutions with different concentrations of 0.5−20% were prepared by heating respective weights of PVA in water at 80 °C and allowing them to cool to room temperature. The heating helps the breaking of self-H-bonding in PVA and enhances the solubility. The adsorption and water flux experiments were carried out by using a stirred cell which is similar to the setup reported earlier by others.[11] The pressure applied was controlled by nitrogen gas. A hydrophobic PVDF membrane was fitted in a magnetically stirred cell and 10 mL of PVA aqueous solutions with different concentrations was added to the cell and was stirred for 15 min. A 0.2 bar pressure was applied to pass PVA solution through the membrane. Different membranes with varying concentrations of PVA were prepared. These adsorbed membranes were washed with deionized water and hot water to remove any unadsorbed polymer on the surface until the permeate showed negligible UV absorbance for PVA in the washed liquid.

2.2. Characterization. Water Flux (Permeation Study). Permeate fluxes of pure water were measured on adsorbed membranes in a stirred cell at 0.6 bar and at room temperature. Dry membrane samples for characterization were treated with 2-propanol and then with hexane followed by vacuum-drying for 24 h.

XPS. XPS was recorded using a VG Microtech Multilab ESCA 3000 spectrometer[21,22] with a nonmonochromatized Al Kα X-ray ($h\nu$ = 1486.6 eV) on virgin PVDF membrane and after PVA adsorption on PVDF membranes. Base pressure in the analysis chamber was maintained at $(3-6) \times 10^{-10}$ mbar range. The energy resolution of the spectrometer was set at 1 eV at a pass energy of 20 eV. Binding energy (BE) was calibrated with respect to Au $4f_{7/2}$ core level at 83.9 eV. The error in all the BE values reported is ±0.1 eV.

Energy-Dispersive X-ray Analysis (EDAX). Bulk composition of both virgin PVDF and PVA adsorbed PVDF membranes was carried out by using EDAX (Phoenix, EDAX international, U.S.A.) at an accelerating voltage of 20 KV.

Mercury Intrusion Porosimetry. Porous properties of the membranes were studied by using mercury intrusion porosimetry (Autoscan-33 mercury porosimeter from Quantachrome, U.S.A.) in the pressure range of 0−33 000 PSIG.

Contact Angle Measurement. Contact angle measurements were carried out with Rame Hart telescopic goniometer and Gilmont syringe.

3. Results and Discussion

3.1. XPS of Carbon 1s Core Level. Figure 1 shows a comparison of carbon 1s core level spectra from untreated PVDF membrane and PVA adsorbed PVDF membranes with different PVA concentrations. The PVDF membranes treated with high (≥10%) and low (≤1%) PVA concentrations do not show uniform PVA adsorption, and patchy surfaces are observed by naked eyes. Further, a change in molecular weight of PVA from 31 to 67 K also does not have significant influence in the binding energy (BE) of any of the elements, except for surface composition (vide infra). PVDF membranes show two carbon features at 286 and 290.6 eV because of CH_2 and CF_2 group carbons, respectively. However, upon treatment with 1% PVA solution for 15 min, a dramatic decrease in CF_2 intensity and a broadening in the CH_2 carbon peak indicated the adsorption of PVA on PVDF. The carbon species at lowest BE (284.7 eV) and at 286 eV is attributed to the all backbone methylene group carbons and carbons attached to oxygen in PVA, respectively. A small peak is discernible at around 288.5 eV. On increasing the PVA concentration to 2%, a further decrease in CF_2 group intensity and a corresponding decrease in the intensity of associated CH_2 group were observed. In the case of 2% PVA adsorption, a peak at 288.5 eV is more clear and it is comparable in intensity to that of the CF_2 group at 290.6 eV. Further enhancement in the PVA concentration up to 4% shows additional changes of lowest CF_2 group intensity and a comparatively higher intensity of the peak at 287.9 eV. Deconvolution was performed to show the individual components for all C 1s peaks. It is assumed for deconvolution that the intensity of CF_2 and the associated CH_2 groups from PVDF should have the same intensity ratio as observed on pure PVDF. The carbons associated with hydroxyl groups in PVA are attributed to the peak at 286.1 eV. The carbonyl carbon from PVA is attributed to the peak between 287.9 and 288.7 eV, and this particular group is suspected to be at the interface between the PVA and PVDF. A considerable decrease in the BE of the above interface on 4% PVA adsorbed membrane clearly indicates that there could be some charge transfer from carbonyl oxygen to PVDF chain, likely through the carbons of CF_2 group since they are electron-deficient.

The higher percentage of PVA adsorbed samples (≥10%) shows an increase in CF_2 and in the corresponding CH_2 group intensity. The interface carbonyl carbon also shifts to a higher BE to 288.7 eV. However, the patchy nonuniform surfaces observed on higher PVA adsorption make the comparison difficult with the results from low-percentage PVA treated (<10%) surfaces. Nonetheless, the qualitative trend observed in our results clearly shows that the higher PVA percentage treatment does not necessarily increase the PVA content on the PVDF surfaces. Apparently, 4% PVA concentration treatment on PVDF displays the maximum PVA adsorption and indicates that there is a threshold PVA coverage on PVDF. This is further confirmed from the above observation of increasing CF_2 intensity ≥5% PVA adsorbed surfaces (vide infra Figure 3). This observation reiterates that it is not just physical multiple deposition of PVA on PVDF but a limited PVA adsorption and

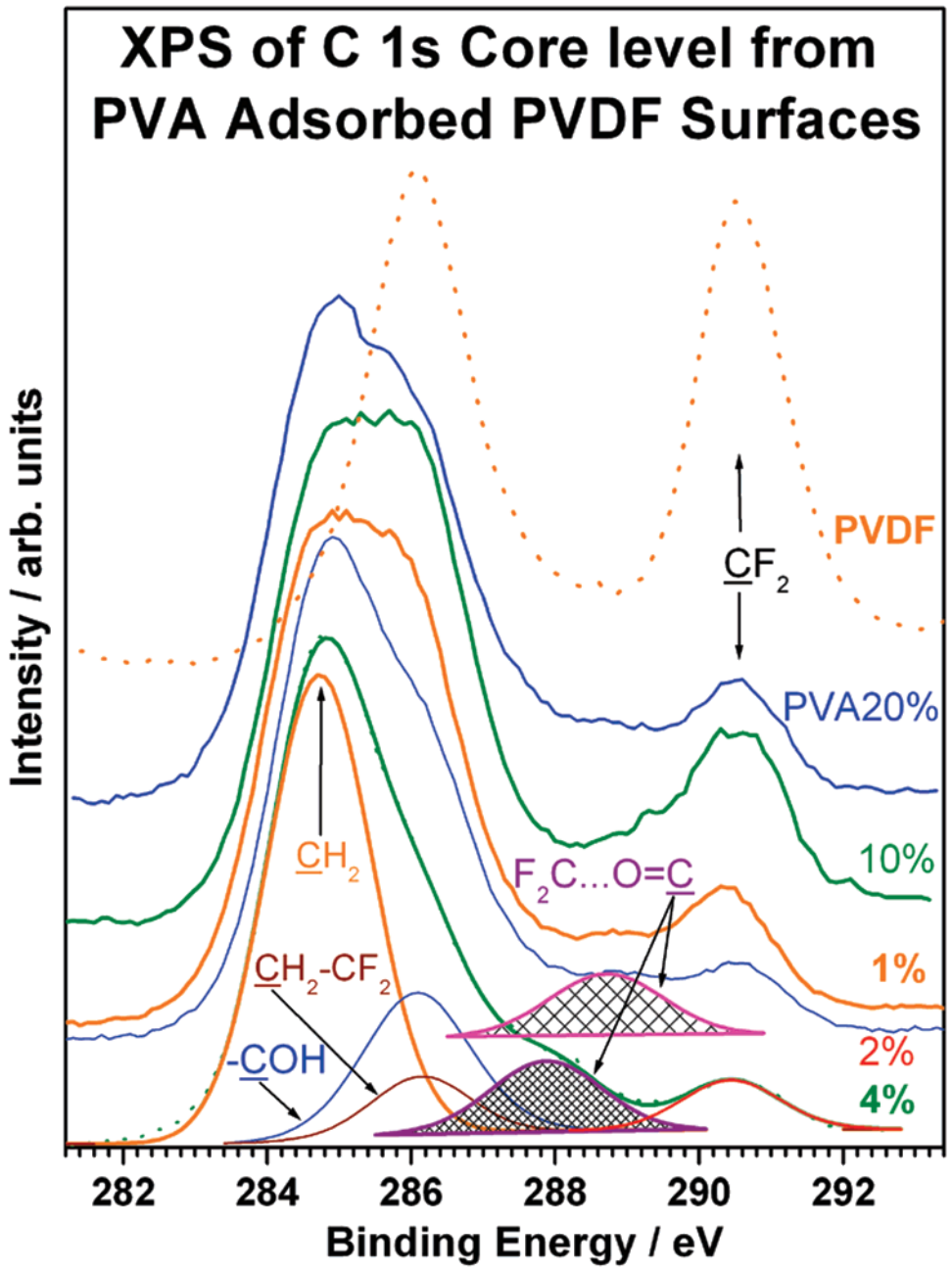

Figure 1. Carbon 1s core level spectra from virgin PVDF and PVA adsorbed PVDF surfaces. C 1s from 4% PVA treated surface is deconvoluted to show the individual peaks and to note the shift in binding energy of carbonyl carbon in it.

a fairly strong interaction between PVA and PVDF. Other core level and valence band studies substantiate our above conclusions.

3.2. XPS of Oxygen 1s Core Level. Figure 2a shows the oxygen 1s core level spectra from PVA adsorbed PVDF membrane surfaces after normalization to 4% PVA adsorbed surfaces. As expected, the virgin PVDF surface does not show any significant oxygen 1s intensity and is not shown in Figure 2a. PVA adsorption with 1, 2, and 10% solution shows oxygen 1s peak at 532.4 eV with a marginal change in full width at half-maximum (fwhm) of 2.3 ± 0.1 eV. However, oxygen 1s from 4% PVA adsorbed surface shows a shift in BE to 531.9 eV and an additional broadening to lower BE with an fwhm = 2.8 eV. This indicates that there is an additional oxygen component, which plays a significant role on 4% PVA adsorbed membranes. Deconvolution of oxygen 1s core level from PVA (1, 2, and 10%) adsorbed PVDF surfaces also shows two peaks with a BE difference of 0.7 eV and the low BE feature appearing at 532 eV. However, 4% PVA surface shows two components at 531.5 and 532.8 eV. Further, the intensity ratio of low to high BE feature is 3:2 for 4% and higher PVA concentration, and it is 3:5 for 1 and 2% PVA adsorbed surfaces. Hence, it is suggested that the oxygen at low BE might be playing a crucial role in the interface formation with PVDF backbone.

3.3. XPS of Fluorine 1s Core Level. Figure 2b shows the fluorine 1s core level spectra from PVDF and PVA adsorbed PVDF membrane surfaces. Virgin PVDF surfaces shows intense F 1s peak at 688.2 eV. However, all PVA adsorbed PVDF membranes show the F 1s peak at 687.7 eV, with different intensities. This clearly indicates that there is a significant increase in the electron density of fluorine because of PVA adsorption, irrespective of the concentration of PVA. F 1s peak intensity decreases, exactly in the same manner as with CF_2 group intensity in C 1s results (Figure 1); the intensity decreases from 1% PVA to 4% PVA and then interestingly it increases above 4% PVA concentration. This result also clearly suggests

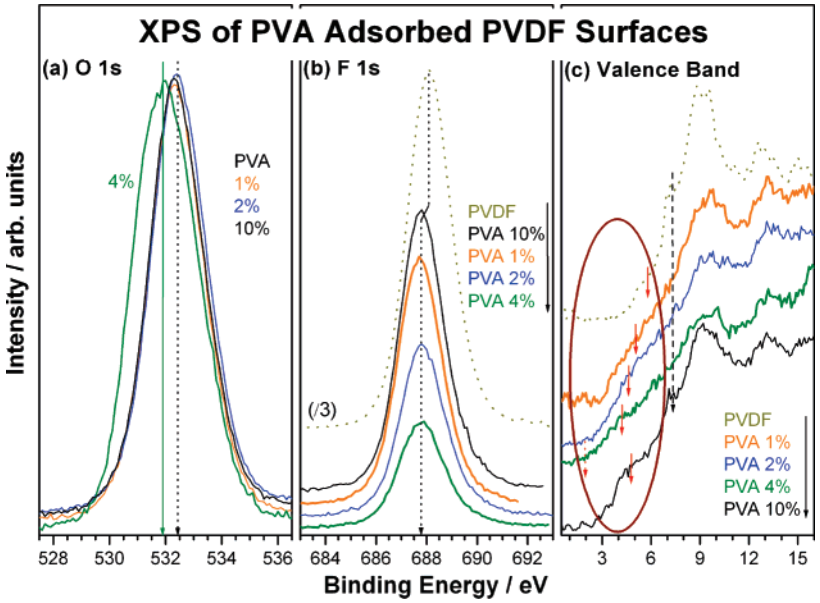

Figure 2. XPS recorded from (a) O 1s core level, (b) F 1s core level, and (c) valence band on virgin PVDF and PVA adsorbed PVDF membrane surfaces.

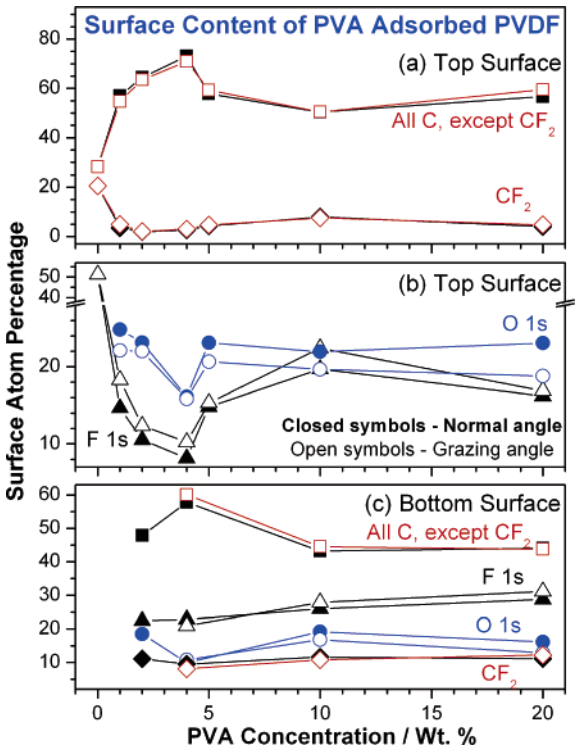

Figure 3. Plots of surface atom percentage measured on top (a and b) and bottom (c) surfaces of PVDF and 31 K PVA adsorbed PVDF membranes from XPS results.

that there exists the threshold coverage of PVA on PVDF and it is about 4%.

3.4. Valence Band XPS Studies. Figure 2c shows the valence band (VB) spectra obtained from PVDF and PVA adsorbed PVDF membrane surfaces. Virgin PVDF membrane shows a small peak around 6 eV and many other bands at 7.3, 8.8, 9.5, 12.9, and 15.2 eV are attributed to F 2p, C 2p, and C 2s derived features.[23] Our VB results on PVDF are in excellent agreement with the earlier ultraviolet photoemission spectral results.[23] The HOMO around 6 eV is from the bonding orbitals of the carbon atoms in the main chain and the antibonding orbitals of the C−F bonds.[23] Upon PVA adsorption on PVDF membranes, there is a development of a new filled band at BE ≤ 5 eV, and it shifts with the increasing percentage of PVA. The shift in the BE of the topmost band is indicated by solid arrows in Figure 2c. Furthermore, the photoemission onset also shifts to lower BE in resonance with the BE of the topmost band, and the lowest onset energy observed at 4% PVA adsorbed surface is at 2 eV (broken arrow). Further increase in PVA concentration increases the BE of the HOMO to higher BE. There is an overall agreement between the VB features from PVDF and PVA adsorbed PVDF membranes in terms of BE; however, the sharpness and the intensity of the bands decrease and start broadening with increasing PVA concentration, and maximum broadened VB features were observed at 4% PVA adsorbed surfaces. An additional increase in PVA concentration again starts showing sharper PVDF features at the same BE as on virgin PVDF. The conductivity measurements, made through the membranes, show an insulating character of PVDF changes upon PVA adsorption, and a resistance value in the range of 60−100 GΩ is observed for any PVA adsorbed PVDF membranes. The positive static charging observed in XPS on PVDF also decreases very significantly upon PVA adsorption. This is in agreement with a decrease in the HOMO energy of PVA adsorbed PVDF membranes.

It is to be noted from the literature that the oxygen 2p derived orbital as well as the unsaturated carbon−carbon bonds here bring in the high density of states of HOMO.[24] From this viewpoint, it is likely that the development of the new filled band below 5 eV, which is also HOMO for PVA adsorbed PVDF surfaces (Figure 2c), should be derived from oxygen 2p features. An increase in the intensity of HOMO of PVDF at 6 eV and a decrease in F 1s core level BE on PVA adsorbed surfaces indicate some electron filling of C−F antibonding band. This suggests a decrease in C−F bonding character at least on the surface and the interface of PVDF and might be a reason for the enhanced and irreversible bonding between PVA and PVDF. Furthermore, certain specific orientation between PVA and PVDF might enhance the extent of adsorption or interaction among them and especially at 4% PVA adsorbed surface the interaction may be the highest. Such geometric alignments between PVA and PVDF are not ruled out for the maximum water permeability (discussed in the foregoing) and for the

special features observed in XPS results also. Molecular modeling studies might throw more light on such orientations and on their effects on properties.

3.5. Surface Concentration of Constituent Elements: Figure 3 shows the surface atom percentage of all the elements analyzed on virgin PVDF and 31 K PVA adsorbed PVDF membranes. Further, the top and bottom surfaces of the membranes are also analyzed at normal emission angle as well as at grazing angle to probe any enhancement of PVA on the surface. Figure 3a shows the carbon atom percentage from CF_2 group carbons and all other carbon atoms clubbed together. This is mainly to show how the PVDF contribution to surface changes with PVA adsorption. Despite the bulk 1:1 ratio of CF_2:CH_2 and C:F on PVDF, a lower amount of surface carbons (20.5%) bonded to fluorine than to CH_2 (28.1%), and a somewhat higher atomic percentage of F (51.4%) than C (48.6%) was observed on the surface. This suggests that the fluorine atoms are projected outward from the surface and carbons are projected toward the subsurface in the C−F bond, and it might be attributed to minimizing the surface energy. Nonetheless, this indicates that the surface is somewhat rich in fluorine and the carbon and fluorine atom percentage ratio is close to 1:1 on PVDF. 1 and 2% PVA adsorbed PVDF membrane surface shows a drastic reduction in the F-content to less than 20% on the surface and a simultaneous increase in the oxygen content of more than 20%. A corresponding decrease in CF_2 group carbon atom percentage also is observed. These observations reiterate that an increase in oxygen atom percentage is exclusively due to PVA adsorption. Independent of PVA concentration, a very significant fluorine atom percentage (8−20%) on PVA adsorbed PVDF surfaces hints that the PVA adsorption is exclusively limited to the surface, which likely is less than the XPS probing depth of about 5 nm. A simple comparison of virgin and 4% PVA adsorbed PVDF displays a change in surface atomic character from predominantly fluorine derived to carbon and oxygen derived surfaces, respectively, due exclusively to PVA adsorption. This is further confirmed from the EDAX analysis of PVA adsorbed PVDF membranes. Irrespective of PVA% and molecular weight (31 K or 67 K), the weight percentage of oxygen varies between $4.5 \pm 0.6\%$, and the carbon ($58 \pm 1\%$) and the fluorine ($38 \pm 0.8\%$) do not change significantly.

The total carbon atom percentage from all other carbons also increases, mainly because of contributions from adsorbed PVA. The 4% PVA adsorbed PVDF membrane shows a further increase in non-fluorocarbon atom percentage and a minimum amount of fluorine content of 8%. Notably, the oxygen atom percentage also decreases to a low level of 16%; however, it is significantly higher than the fluorine content. A careful comparison of all atom percentages reveals that the non-fluorocarbon content is highest and that the other atom percentages are at their lowest on 4% PVA adsorbed surfaces, and this might be due to rearrangement of methylene backbones of PVA to an optimal configuration. A further increase in PVA percentage decreases the non-fluorocarbon percentage, and it shows around 60% for all higher PVA levels. However, the fluorocarbon and the fluorine content maintains between 4 and 7% and between 15 and 20%, respectively, at high PVA levels. The oxygen percentage was maintained around 22−24% for all high PVA adsorbed PVDF membranes, and this also indicates that the excess PVA was not adsorbed on the PVDF surfaces and that PVA adsorption is limited to the surface.

The above measurements made at grazing emission angle revealed some changes in the atom percentage on the surfaces compared to normal emission, especially with F and O atoms at low PVA levels. About a 3% decrease in oxygen at grazing angle compared to normal and to the same extent an increase in fluorine at grazing angle compared to normal on 1% PVA adsorbed PVDF membranes reveal that the PVA amount is not sufficient to fully cover the PVDF surfaces and it is likely that there may be some portions of PVDF membrane without any PVA adsorbed on it. The difference between normal and grazing angle decreases with increasing PVA% up to 4%. Oxygen content does not show any difference between normal and grazing emission angle on 4% PVA adsorbed membranes with lowest F-content indicating that all PVDF pores are likely adsorbed with PVA for a few monolayers, within the probing depth of about 5 nm in XPS. It is needless to state that the top surface layers are highly crucial in determining the wettability of any surfaces. A further increase in PVA% reverses the trend that is observed below 4%. This behavior is attributed to the viscous nature of PVA at higher percentage, which might prevent efficient PVA adsorption on PVDF membrane surfaces.

Selected PVA adsorbed PVDF membrane surfaces were analyzed on the bottom surfaces also to see the change in atomic content. About 10−17% oxygen content and 20−30% fluorine content definitely indicates that PVA got adsorbed throughout the bulk surfaces of the PVDF membrane. However, the higher percentage and hence the viscous PVA hinder its diffusion and adsorption on PVDF, and hence there is a higher percentage of F and fluorocarbon on the bottom surfaces. However, some amount of PVA adsorption throughout the bulk surfaces is obtained even with viscous PVA solutions. Our EDAX analysis also confirms the same.

3.6. Membrane Texture Properties. Compared to untreated PVDF membranes, changes in pore size, pore size distribution, pore volume, and surface area are expected for the PVA adsorbed PVDF membranes. Some of the representative membranes were subjected to mercury porosimetry analysis, and the results are shown in Figure 4. Differential pore volume to pressure (dV/dP), cumulative surface area, and pore number fraction are plotted against the pore size distribution in Figure 4a, b, and c, respectively, for PVDF (blue-dotted), 31 K PVA 4% (orange), and 67 K PVA 4% (green) adsorbed on PVDF membranes. Differential pore volume to pressure indicates that the micropore size decreases a significant extent but not dramatically upon PVA adsorption. However, the two intermediate size pores of 0.015 and 0.03 μm on PVDF membrane disappear completely after PVA adsorption. Besides, it creates a range of nanopores in the membrane (dotted box in Figure 4a). Some of the above points are affirmed from the observation of the same extent of cumulative surface area found from micropores before and after PVA adsorption. However, the main reason for high surface area on virgin PVDF membrane is due to intermediate pores. PVA adsorption should have been really effective on these pores and, hence, the size of these pores shrinks greatly to nanopore sizes (Figure 4b). However, the nanopores created after PVA adsorption contribute in a major way to an increase in surface area. Originally, there were no nanopores available on the virgin PVDF membranes.

The pore number fraction measured also indicates that the micropore sizes reduced significantly with both 31 K and 67 K PVA adsorption. A definite decrease in pore size, from 0.22 μm on PVDF to 0.13 μm, is evident after PVA adsorption compared to virgin PVDF (see dotted box in Figure 4c). Creation of nanopores is also evident and contributes to the maximum for pore number fraction. Furthermore, nanopores with certain sizes (5.5, 8, and 13 nm) are completely absent on 67 K PVA

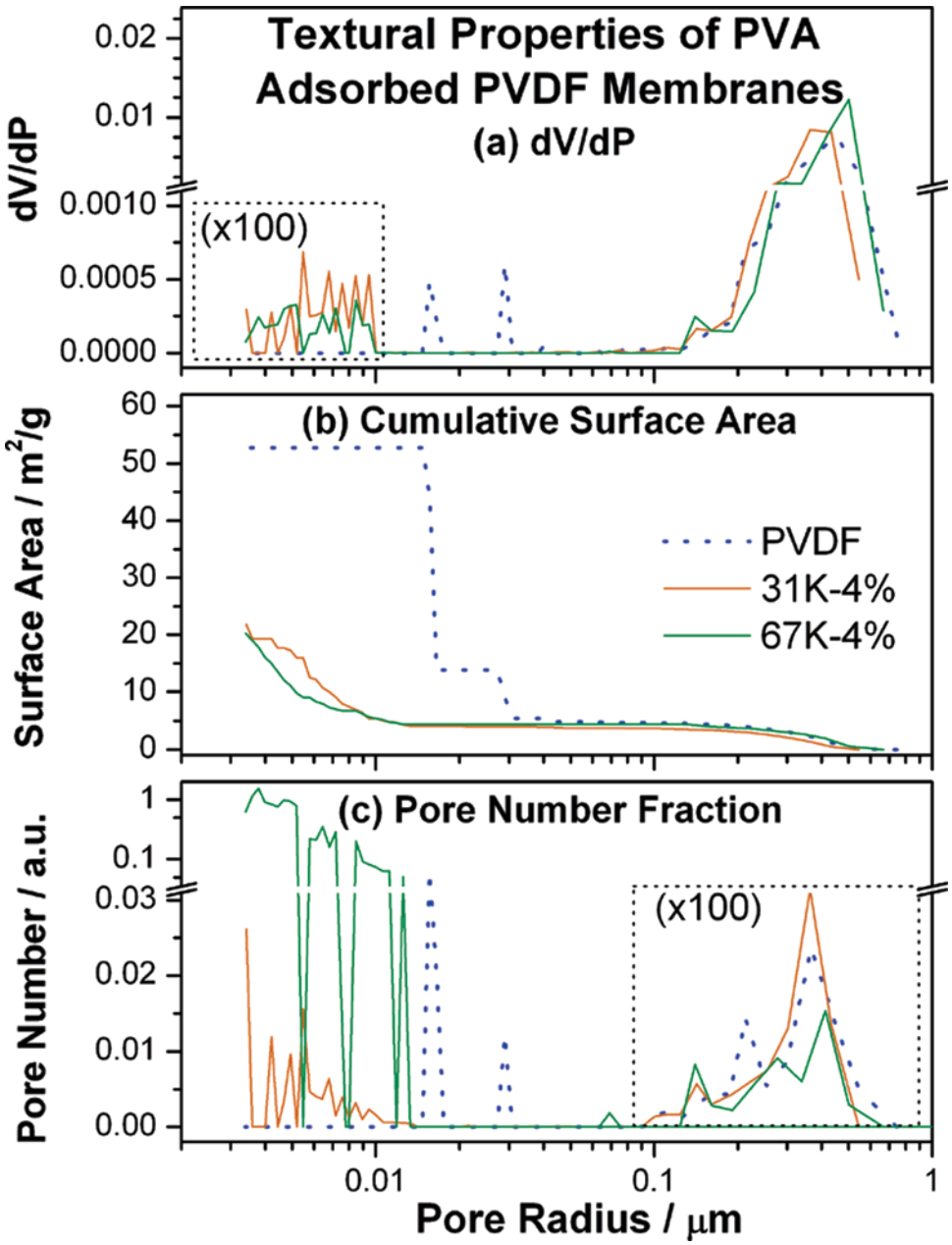

Figure 4. Textural properties measured from mercury porosimeter are plotted against pore radius of PVDF and PVA on PVDF membranes. (a) Differential pressure to differential volume change, (b) surface area, and (c) pore number fraction.

adsorbed surface, which indicates that there could be some preferred alignments of alkyl chains. Molecular modeling studies might shed light on this matter, but this is beyond the scope of the present work. The above textural properties before and after PVA adsorption on PVDF mainly suggest that the PVA adsorption preferentially takes place on intermediate pores on PVDF and then on micropores. The different alkyl chain lengths in 31 K and 67 K PVA have some effect on textural properties.

3.7. Water Permeation Studies. The untreated PVDF membranes are microporous and highly hydrophobic in nature. Therefore, they did not show any water permeation at 0.6 bar. However, hydrophilizing them with PVA showed high water permeation. We show in Figure 5 the water permeation of PVDF membranes treated with PVA (31 K) of different concentrations. It can be readily seen that the water flux increases and is maximum for PVDF membranes treated with 4% PVA and then there is a marginal decrease with increasing PVA%. This also supports the existence of a threshold coverage of PVA on PVDF at 4% concentration. The increase in water flux is attributed to the increase in hydrophilicity of the PVDF membranes. The increase in hydrophilicity was further confirmed by contact angle measurements. The quantitative measurement of the contact angle was limited by the porous nature of the PVDF membrane. The irreversible adsorption of PVA on PVDF is intriguing and perhaps can be considered as the simplest method of converting hydrophobic membranes into hydrophilic membranes. The membrane textural properties indicated the change in size of intermediate pores after adsorption of PVA. The critical balance of PVA concentration on the PVDF membranes and the pore size can influence the permeability of membranes.

A comparison of Figures 3 and 5 reveals that the water permeability increases somewhat linearly with an increase in carbon content (except fluorocarbons) (Figure 3a). Similarly, the water permeability and fluorine content on the surface displays an inverse but linear trend. However, such a relation is not obvious between oxygen content and water permeability because of a very small amount of oxygen in the PVA molecule. This also indicates that the diminishing fluorine content and an

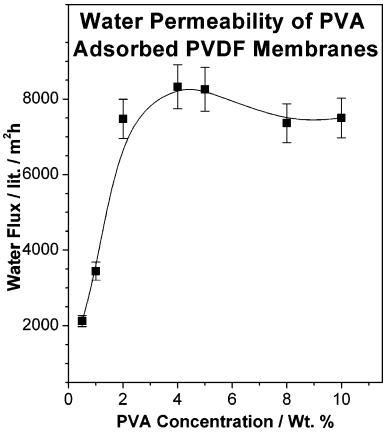

Figure 5. Rate of water permeability on PVA (31 K) adsorbed PVDF membranes at 0.6 bar.

optimally adsorbed PVA content on the surface might be equally important for water permeability in the present case.

4. Conclusions

Molecular origins of wettability of irreversibly adsorbed PVA on PVDF membranes have been explained mainly through surface and interface analysis by XPS. An interface formation between PVA and PVDF was demonstrated, and it is likely due to the interaction between the carbonyl group of PVA and the CF_2 group of PVDF backbone. Likely, there is some charge transfer from PVA to PVDF, and a decrease in F 1s BE suggests a reduction in C−F bonding character upon PVA adsorption. A new highest occupied valence band observed on PVA adsorbed PVDF membranes clearly indicates that the nature of the topmost orbitals/bands changes from mostly F and C on PVDF to oxygen derived on PVA adsorbed membranes and, hence, to a change in hydrophobic to hydrophilic character. This is further supported from the surface atomic content of PVDF and PVA adsorbed PVDF membranes. Water permeability studies on the membranes show a maximum permeability with 4% PVA concentration adsorbed PVDF membrane. XPS studies and water permeability experiments indicate that the threshold value is 4%. There is also a considerable change in textural properties of the adsorbed membranes, which supports our conclusions.

Acknowledgment. Shubhangi G. Gholap acknowledges the CSIR, New Delhi, for the grant of a senior research fellowship. We thank Dr. S. Sivaram (Director, NCL) for his constant encouragement to take up interdivisional collaborations.

References and Notes

(1) Nabe, A.; Staude, E.; Belfort, G. *J. Membr. Sci.* **1997**, *133*, 57.
(2) Belfer, S.; Gilron, J.; Purinson, Y.; Fainshtain, R.; Daltrophe, N.; Priel, M.; Tenzer, B.; Toma, A. *Desalination* **2001**, *139*, 169.
(3) Gancarz, I.; Pozniak, G.; Bryjak, M. *Eur. Polym. J.* **2000**, *36*, 1563.
(4) Kim, K. S.; Lee, K. H.; Cho, K.; Park, C. E. *J. Membr. Sci.* **2002**, *199*, 135.
(5) Wavhal, D. S.; Fisher, E. R. *Langmuir* **2003**, *19*, 79.
(6) Wang, P.; Tan, K. L.; Kang, E. T.; Neoh, K. G. *J. Membr. Sci.* **2002**, *195*, 103.
(7) Ulbricht, M.; Belfort, G. *J. Membr. Sci.* **1996**, *111*, 193.
(8) Akhtar, S.; Hawes, C.; Dudley, L.; Reed, I.; Stratford, P. *J. Membr. Sci.* **1995**, *107*, 209.
(9) Stengaard, F. F. *Desalination* **1988**, *70*, 207.
(10) Hvid, K. B.; Nielsen, P. S.; Stengaard, F. F. *J. Membr. Sci.* **1990**, *53*, 189.
(11) Na, L.; Zhongzhou, L.; Shuguang, X. *J. Membr. Sci.* **2000**, *169*, 17.
(12) Uyama, Y.; Kato, K.; Ikada, Y. *Adv. Polym. Sci.* **1998**, *137*, 1.
(13) Kato, K.; Uchida, E.; Kang, E.-T.; Uyama, Y.; Ikada, Y. *Prog. Polym. Sci*. **2003**, *28*, 209.
(14) Shoichek, M. S.; McCarthy, T. J. *Macromolecules* **1991**, *24*, 1441.
(15) Kozlov, M.; Quarmyne, M.; Chen, W.; McCarthy, T. J. *Macromolecules* **2003**, *36*, 6054.
(16) Serizawa, T.; Hashiguchi, S.; Akashi, M. *Langmuir* **1999**, *15*, 5363.
(17) Coupe, B.; Chen, W. *Macromolecules* **2001**, *34*, 1533.
(18) Nash, D. C.; McCreath, G. E.; Chase, H. A. *J. Chromatogr., A* **1997**, *758*, 53.
(19) Witt, J. A. De; Ven, T. G. M. van de *Langmuir* **1992**, *8*, 788.
(20) Barette, D. A.; Hartshorne, M. S.; Hussain, M. A.; Shaw, P. N.; Davies, M. C. *Anal. Chem.* **2001**, *73*, 5232.
(21) Waghmode, S.; Vetrivel, R.; Gopinath, C. S.; Sivasanker, S. *J. Phys. Chem. B* **2003**, *107*, 8517. Velu, S.; Suzuki, K.; Gopinath, C. S. *J. Phys. Chem. B* **2002**, *106*, 12737.
(22) Mathew, T.; Shiju, N. R.; Bokade, V. V.; Rao, B. S.; Gopinath, C. S. *Catal. Lett.* **2004**, *94*, 223.
(23) Morikawa, E.; Choi, J.; Manohara, H. M.; Ishii, H.; Seki, K.; Okudaira, K. K.; Ueno, N. *J. Appl. Phys.* **2000**, *87*, 4010.
(24) Maehl, S.; Neumann, B.; Schneider, B.; Schlett, V.; Baalmann, A. *J. Polym. Sci., Part A* **1999**, *37*, 95.